Proc. Natl. Acad. Sci. USA
Vol. 93, pp. 11664–11668, October 1996
Cell Biology

Microtubules mediate mitochondrial distribution in fission yeast

(cytoskeleton/*Schizosaccharomyces pombe*/organelle movement)

MICHAEL P. YAFFE*†, DAI HARATA‡§, FULVIA VERDE§¶, MARK EDDISON‡, TAKASHI TODA‡, AND PAUL NURSE¶

*Department of Biology, 0347, University of California at San Diego, La Jolla, CA 92093; and ‡Cell Regulation Laboratory and ¶Cell Cycle Laboratory, Imperial Cancer Research Fund, 44 Lincoln's Inn Fields, London, WC2A 3PX, United Kingdom

Communicated by Giuseppe Attardi, California Institute of Technology, Pasadena, CA, July 1, 1996 (received for review April 15, 1996)

ABSTRACT **The *Schizosaccharomyces pombe* mutant, *ban5-4*, displays aberrant mitochondrial distribution. Incubation of this conditional-lethal mutant at the nonpermissive temperature led to aggregated mitochondria that were distributed asymmetrically within the cell. Development of this mitochondrial asymmetry but not mitochondrial aggregation required progression through the cell division cycle. Genetic analysis revealed that *ban5-4* is an allele of *atb2* encoding α2-tubulin. Consistent with this finding, cells with the cold-sensitive *nda3* mutation in β-tubulin displayed aggregated and asymmetrically distributed mitochondria after incubation at lowered temperatures. These results indicate that microtubules mediate mitochondrial distribution in fission yeast and provide the first genetic evidence for the role of microtubules in mitochondrial movement.**

The cytoskeleton is thought to mediate the distribution of mitochondria within eukaryotic cells. In particular, a number of studies have implicated microtubules in the movement and positioning of mitochondria. Mitochondria exhibit saltatory motion, characteristic of movement along microtubules or other cytoskeletal structures (1, 2). Frequently, mitochondria display a subcellular distribution corresponding to that of specific cytoskeletal components, particularly to the cytoplasmic microtubular network (3–5). Treatment of cultured animal cells with chemical agents that depolymerize microtubules often leads to altered mitochondrial distribution (3, 6). Filamentous cross-bridges between mitochondria and microtubules have been detected by electron microscopy of frozen frog neurons (7). Finally, an isozyme of the microtubule-based motor protein kinesin has been localized to mitochondria in neuronal cells (8).

Despite numerous correlations between mitochondrial distribution and the microtubule network, genetic evidence of a role for microtubules in mitochondrial positioning has been lacking. In several unicellular organisms, genetic analysis has failed to corroborate a role for microtubules in mitochondrial movement. In the budding yeast, *Saccharomyces cerevisiae*, neither mutations nor chemical agents that disrupt microtubule function appear to affect either mitochondrial distribution or the movement of mitochondria into developing buds (9, 10). Mitochondrial movement is similarly unaffected by mutations in β-tubulin in cells of the filamentous fungus, *Aspergillus nidulans* (11).

We have screened a collection of mutants of the fission yeast *Schizosaccharomyces pombe* to identify strains defective for mitochondrial distribution. Such an approach previously identified mitochondrial inheritance mutants in the budding yeast, *Sac. cerevisiae* (12, 13). Each strain in the *Sch. pombe* mutant collection possessed a temperature-sensitive lesion causing either aberrant cell morphology (14–16) or a block in progression through the cell division cycle (17, 18). Analysis of one of these mutant strains has revealed the dependence of mitochondrial distribution on the cytoplasmic microtubule network.

MATERIALS AND METHODS

Yeast Strains and Genetic Analysis. *Sch. pombe* strains used included the wild-type strain (*leu1-32, h⁻*), single temperature-sensitive mutant strains *ban5-4* (*leu1-32, h⁺*), *ban5-996* (*leu1-32, h⁻*), *cdc25-22* (*h⁺*), and *nda3-311* (*leu1-32, h⁻*), and double mutant strains *ban5-4 cdc2-33*, *ban5-4 cdc10-129*, *ban5-4 cdc20-M10*, and *ban5-4 cdc7-24*. Cells were cultured on YE medium (0.5% yeast extract/3% glucose) or YPD medium (1% yeast extract/2% bactopeptone/2% glucose). Genetic manipulations and analysis were performed by standard procedures (19).

Microscopic Analysis. For the visualization of mitochondria in live *Sch. pombe* cells, a 0.2 ml sample was mixed with 30 μl of a solution of 0.5 mg/ml 2-(4-dimethylaminostyryl)-1-methylpyridinium iodide (DASPMI; Sigma) in water and incubated at 36°C for 5 min. Cells were recovered by centrifugation in a microcentrifuge for 2 min at low speed, resuspended in 0.2 ml YE medium, and examined immediately with the fluorescence microscope. Calcofluor staining was done as described (16). For indirect immunofluorescence microscopy, cells were collected by centrifugation at 1500 × *g* for 2 min and fixed in methanol at −20°C for 20 min. Samples were processed for indirect immunofluorescence microscopy as described (20). Mitochondria were visualized using a mouse monoclonal antibody specific for mitochondrial HSP-60 (Clone LK2; Sigma) and rhodamine-conjugated goat anti-mouse secondary antibody (Jackson ImmunoResearch) or with affinity-purified (21) rabbit antibody directed against the β-subunit of the mitochondrial F_1-ATPase (22) and fluorescein-conjugated, affinity-purified, goat anti-rabbit immunoglobulin (Jackson ImmunoResearch). Microtubules were detected with a mouse monoclonal antibody against α-tubulin [TAT-1 (23), provided by Keith Gull] and either Cy3-conjugated goat anti-mouse IgG (Sigma) or rhodamine-conjugated, affinity-purified, donkey anti-mouse immunglobulin (Jackson ImmunoResearch) as the secondary antibody.

RESULTS AND DISCUSSION

To screen for *Sch. pombe* cells displaying mitochondrial distribution defects, individual mutant strains possessing temperature-sensitive defects in either cell morphology (14–16) or the cell division cycle (17, 18) were cultured at the permissive temperature, 25°C, incubated for 4 h at the nonpermissive temperature, 36°C, and examined by fluorescence microscopy after staining with the mitochondria-specific vital dye DASPMI (24, 25). Mitochondria in wild-type cells and in most

The publication costs of this article were defrayed in part by page charge payment. This article must therefore be hereby marked "*advertisement*" in accordance with 18 U.S.C. §1734 solely to indicate this fact.

Abbreviation: DASPMI, 2-(4-dimethylaminostyryl)-1-methylpyridinium iodide.

†To whom reprint requests should be addressed.

§D.H. and F.V. contributed equally to this work.

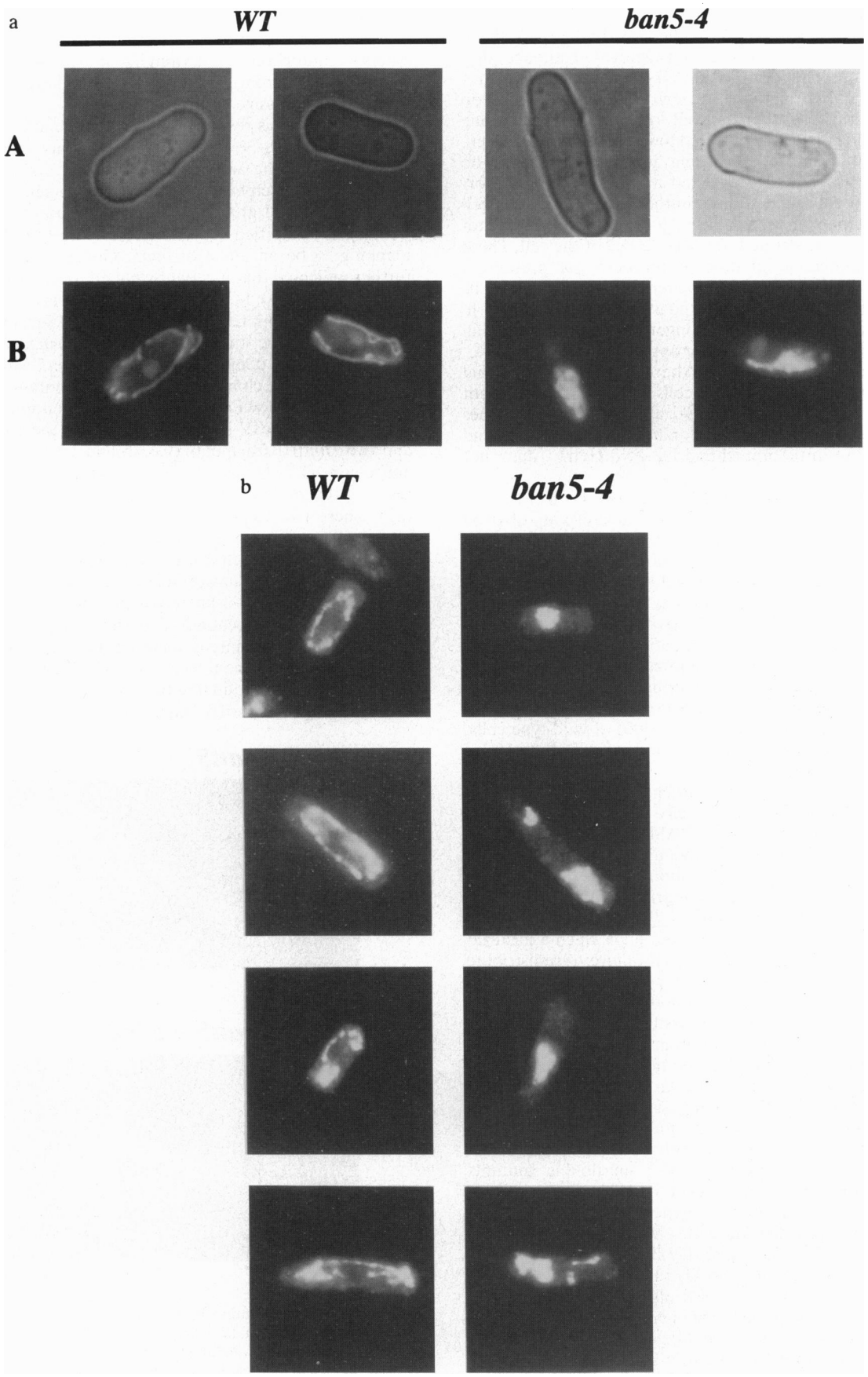

FIG. 1. Aberrant mitochondrial distribution in *ban5-4* mutant cells. (*a*) Cultures were incubated at 36°C for 5 h, stained with DASPMI, and viewed by fluorescence microscopy. Shown are phase-contrast (*A*) and fluorescence (*B*) images of two representative wild-type and two representative *ban5-4* cells. (*b*) Cultures were incubated for 5 h at 36°C, fixed, and analyzed by indirect immunofluorescence microscopy. Four representative cells are shown for wild-type and the *ban5-4* mutant.

of the mutant strains appeared as extended tubules and tubular networks spanning the length of the cell (Fig. 1*a*). A single mutant strain, *ban5-4*, displayed both aggregated mitochondria and marked mitochondrial asymmetry (Fig. 1*a*). The aggregation of mitochondria was characterized by the redistribution of mitochondria from their normal location, extended along the cell periphery and concentrated toward the ends of the cell, to a more disorganized clumping in the cytoplasm. The mitochondrial asymmetry reflected a change from the normally symmetrical distribution of mitochondria within the cell to an arrangement in which the majority or all of the mitochondria were concentrated toward one end of the cell. These changes in mitochondrial distribution were not present in *ban5-4* cells incubated at permissive temperature. Mutant cells shifted to 36°C exhibited aggregated mitochondria within 1 h. Mitochondrial asymmetry took longer to develop, becoming apparent in a fraction of cells after approximately 3 h at 36°C, and in a majority of cells by 5 h. Alterations in mitochondrial distribution were observed also in cells harboring two different mutant alleles, *ban5-3* and *ban5-996*, although the phenotypes appeared less severe, with mitochondrial disorganization and aggregation but little mitochondrial asymmetry (data not shown).

Altered mitochondrial distribution in *ban5-4* cells was confirmed by indirect immunofluorescence microscopy of fixed cells (Fig. 1*b*). Prior to incubation at elevated temperature, >94% (n = 400) of mutant cells contained mitochondria indistinguishable from those of wild-type cells. After 3-h incubation at 36°C, 85% (n = 400) of *ban5-4* cells possessed aggregated mitochondria and 23% (n = 400) displayed mitochondrial asymmetry. After 5 h incubation at 36°C, the fraction of mutant cells with aggregated mitochondria remained constant (85%) while the fraction exhibiting mitochondrial asymmetry increased to 77% (n = 400). Mitochondrial aggregations were detected in fewer than 5% (n = 400) of wild-type cells, and mitochondrial asymmetry was found in fewer than 1% of the wild-type population.

The positions of asymmetric mitochondrial aggregates relative to the polarity of the *Sch. pombe* cells were analyzed by examining cells stained with both DASPMI and calcofluor, an agent that stains the cell wall and distinguishes "old" and "new" ends of the cell (26). Among *ban5-4* cells which displayed a high degree of mitochondrial asymmetry after 5 h at the nonpermissive temperature, 73% (n = 200) possessed mitochondria predominantly in the old ends. Such a localization is consistent with at least a partial failure to redistribute mitochondria during the mitotic cell cycle.

To investigate the origin of mitochondrial asymmetry in the mutant cells, mitochondrial distribution was examined in *ban5-4* cells that were blocked in progression through the cell cycle. Mutant cells incubated at the nonpermissive temperature in the presence of hydroxyurea, an agent that retards cells in S-phase by inhibiting DNA synthesis, did not exhibit mitochondrial asymmetry. In contrast, mitochondria became aggregated in >90% of the treated cells. Mitochondrial asymmetry also failed to develop at 36°C in double mutants possessing both *ban5-4* and a second temperature-sensitive lesion in any one of four different genes required for progression through the cell division cycle. Mutations that blocked progression through S phase [*cdc10-129* and *cdc20-M10* (18)], impeded cells predominantly in G_2 phase [*cdc2-33* (17)], or prevented septation [*cdc7-24* (17)] all blocked the development of mitochondrial asymmetry in *ban5-4* mutants at 36°C. Aggregations of mitochondria were detected in fewer than 5% of the double mutant cells prior to a shift to 36°C, but were readily apparent in >80% of the cells harboring *ban5-4* and any of the four *cdc* mutations after 3 h at the elevated temperature. After 5 h at 36°C, >85% of the double mutant cells displayed aggregated mitochondria. These results suggest that the development of mitochondrial asymmetry in *ban5-4* cells requires progression through an entire cell cycle including cell division. This conclusion is consistent with the appearance of extensive mitochondrial asymmetry in *ban5-4* cells only after 3–5 h (corresponding to more than one cell cycle) after a shift to the nonpermissive temperature.

Genetic analysis revealed that *ban5* is an allele of *atb2*, the gene encoding the α2-tubulin subunit. This identity was revealed through the analysis of *Sch. pombe* strains isolated in another visual screening of temperature-sensitive mutants displaying altered growth polarity (*alp* mutants). One mutation, *alp2*, identified in this screen was found by genetic mapping to be an allele of *ban5*. Genetic mapping of *alp2* further indicated that it is tightly linked to *atb2* which encodes α2-tubulin (27, 28). In addition, multicopy plasmids containing the $atb2^+$ gene suppressed the temperature sensitivity of *ban5* cells. Furthermore, the allelism between *ban5/alp2* and *atb2* was confirmed by demonstrating that the *ban5-996* mutation is located within the cloned DNA fragment containing the $atb2^+$ gene with the following experiment. The genomic $atb2^+$ gene contains one *Hin*dIII site in the middle of the coding region, and two *Hin*dIII fragments (0.6 kb and 1.3 kb) comprise the entire gene (27). Neither of these two fragments is capable of rescuing the *atb2* mutant when carried on high-copy plasmids (27). These two fragments were cloned individually into an integration vector containing a *LEU2* marker gene (28), and Leu^+ integrants, which arose via homologous recombination of the *atb2* sequences, were isolated. Seven of 27 independent integrants with the 1.3-kb fragment were found to suppress both growth and mitochondrial distribution phenotypes of the *ban5-996* mutant, whereas none of the 7 (other) integrants with the 0.6-kb fragment were Ts^+. This result indicates that *ban5* is allelic to *atb2* and that the *ban5-996* mutation is located within the 1.3-kb *Hin*dIII fragment.

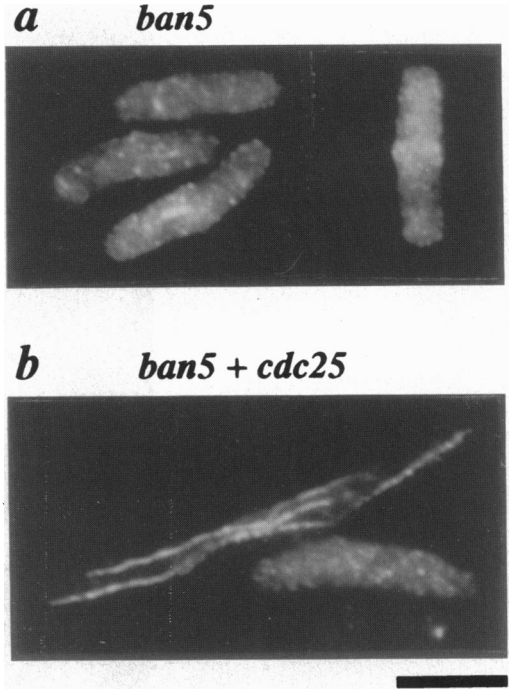

FIG. 2. Indirect immunofluorescence microscopy of microtubules in the *ban5/alp2* mutant. (*a*) Cultures of *ban5-996* cells were incubated at 35.5°C for 4 h, fixed, and analyzed by indirect immunofluorescence microscopy. Four representative cells are shown. (*b*) Cultures of the *ban5-996* and *cdc25-22* mutant cells were incubated for 4 h at 35.5°C, mixed together, and immediately processed for indirect immunofluorescence microscopy. A representative *cdc25-22* (*Upper*) cell and *ban5-996* (*Lower*) cell are shown. An equal number of *ban5-996* and *cdc25-22* cells were mixed before fixation. (Bar = 10 μm.)

Consistent with genetic demonstration of the identity *ban5/alp2* with *atb2*, cytoplasmic microtubules disappeared after a shift of *ban5/alp2* cells to restrictive conditions. Cytoplasmic microtubules were detected in 82% of cells prior to the temperature shift but were found in only 12% of the population after 3 h at 35.5°C. Instead of normal microtubule staining, a discrete punctate pattern was observed in 87% of the cells (Fig. 2*a*). In a small fraction of cells (1%), short mitotic spindles remained. The disappearance of microtubular structures in the *ban5* mutant was confirmed by a mixing experiment in which cells of two different mutant strains, namely *ban5-996* and G_2-arrested *cdc25-22*, were combined prior to fixation for indirect immunofluorescence microscopy. The arrested *cdc25-22* cells were elongated and contained long cytoplasmic microtubules (Fig. 2*b Upper*), whereas the shorter *ban5-996* cells displayed only a punctate pattern (Fig. 2*b Lower*). A similar microtubule staining pattern was observed by indirect immunofluorescence microscopy of *ban5-4* cells; however, mitotic spindle microtubules appeared to persist in some cells for up to 5 h at the restrictive temperature (data not shown). These residual microtubules may mediate nuclear movements and even nuclear division which could contribute to the development of mitochondrial asymmetry.

To investigate further the requirement for microtubules in facilitating mitochondrial distribution, mitochondria were examined in cells harboring the *nda3-311* mutation in β-tubulin (29). Microtubule function is disrupted when this cold-sensitive mutant is incubated at the nonpermissive temperature of 20°C (30). To characterize mitochondrial distribution in the *nda3-311* mutant, indirect immunofluorescence microscopy was performed on cells fixed after a 4-h incubation at 20°C. Mitochondria were aggregated in 91% (n = 400) of the mutant cells, and asymmetric mitochondrial distribution, resembling that observed in *ban5-4* cells, was evident in 22% (n = 400) of the cells (Fig. 3). Mitochondrial distribution and morphology appeared normal in *nda3-311* cells incubated at the permissive temperature, 30°C. In addition, mitochondrial aggregation and disorganization were observed when wild-type cells were treated with the antimicrotubule agent, thiabendazole, and little change in mitochondrial distribution was observed when *nda3-311* cells, which possess microtubules that are largely resistant to this drug (31), were treated at the permissive temperature (data not shown). These results confirm a role for microtubules in the distribution of mitochondria in *Sch. pombe* cells.

Our genetic studies provide strong causal evidence that microtubules mediate the distribution of mitochondria in fission yeast. This involvement of microtubules in mitochondrial positioning was indicated by the behavior of mitochondria in two distinct mutants each disrupted for microtubule function. Consistent with the proposed role for microtubules, double-label indirect immunofluorescence microscopy indicated that a substantial fraction of the mitochondria in wild-type *Sch. pombe* cells was aligned with cytoplasmic microtubules (Fig. 4). A similar alignment has been observed in higher eukaryotic cells (3–5) as well as in the filamentous fungus, *Neurospora crassa* (32). This association of mitochondria with microtubules is in striking contrast to the situation in *Sac. cerevisiae*, where there appears to be no correlation between the positions of these two cellular structures. A relevant difference between *Sch. pombe* and *Sac. cerevisiae* may be the absence in the latter yeast of an elaborate network of cytoplasmic microtubules (20, 33, 34).

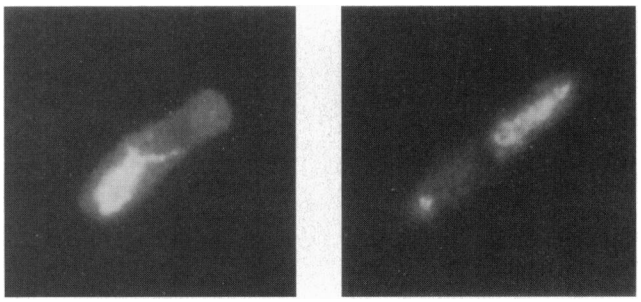

FIG. 3. Aberrant mitochondrial distribution in *nda3-311* mutant cells. Cultures were incubated for 4 h at 20°C, fixed, and analyzed by indirect immunofluorescence microscopy. Two *nda3-311* cells displaying mitochondrial aggregation and asymmetry are shown. Wild-type cells (not shown) appeared identical to those in Fig. 1*b*.

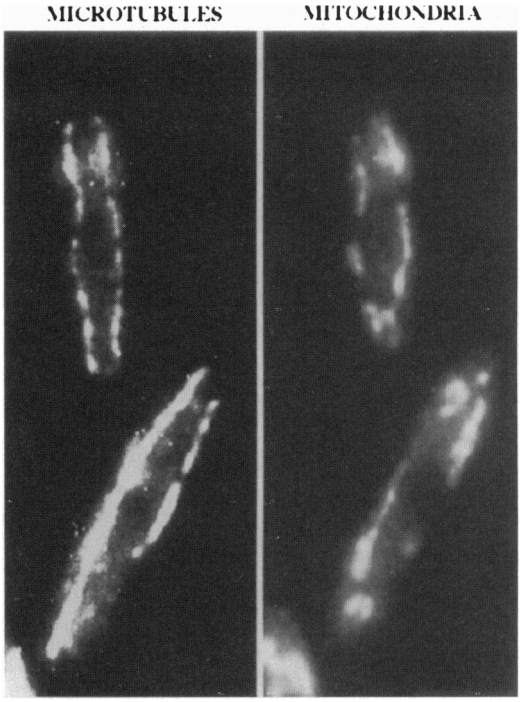

FIG. 4. Alignment of mitochondria with cytoplasmic microtubules. Wild-type *Sch. pombe* cells were fixed and analyzed by double-label indirect immunofluorescence microscopy. No crossover fluorescence between channels was detected in control experiments in which only one of two primary or secondary antibodies was applied to samples (not shown).

The association of mitochondria and microtubules in fission yeast may reflect the activity of the microtubule-based motor proteins kinesin and cytoplasmic dynein (35), which may bind to the mitochondrial surface and both extend and disperse mitochondria along cytoplasmic microtubules. To date, only a single kinesin, the cut7 protein, which is associated with the mitotic spindle, has been identified in *Sch. pombe* (36). However, as in other organisms (37), fission yeast are likely to possess multiple kinesin isozymes as well as dynein species. The sophisticated genetic techniques available for *Sch. pombe* should facilitate the identification of additional motor proteins and a molecular dissection of their roles in mediating the distribution of cellular constituents.

We thank K. Berger for critical reading of the manuscript. This work was supported in part by grants from the National Institutes of Health and the National Science Foundation (to M.P.Y.).

1. Adams, R. J. (1982) *Nature (London)* **297,** 327–329.
2. Aufderheide, K. J. (1977) *Science* **198,** 299–300.
3. Heggeness, M. H., Simon, M. & Singer, S. J. (1978) *Proc. Natl. Acad. Sci. USA* **75,** 3863–3866.
4. Couchman, J. R. & Rees, D. A. (1982) *Eur. J. Cell Biol.* **27,** 47–54.
5. Summerhayes, I. C., Wong, D. & Chen, L. B. (1983) *J. Cell Sci.* **61,** 87–105.

6. Ball, E. H. & Singer, S. J. (1982) *Proc. Natl. Acad. Sci. USA* **79,** 123–126.
7. Hirokawa, N. (1982) *J. Cell Biol.* **94,** 129–142.
8. Nangaku, M., Sato-Yoshitake, R., Okada, Y., Noda, Y., Takemura, R., Yamazaki, H. & Hirokawa, N. (1994) *Cell* **79,** 1209–1220.
9. Jacobs, C. W., Adams, A. E. M., Szaniszlo, P. J. & Pringle, J. R. (1988) *J. Cell Biol.* **107,** 1409–1426.
10. Huffaker, T. C., Thomas, J. H. & Botstein, D. (1988) *J. Cell Biol.* **106,** 1997–2010.
11. Oakley, B. R. & Reinhart, J. E. (1985) *J. Cell Biol.* **101,** 2392–2397.
12. McConnell, S. J., Stewart, L. C., Talin, A. & Yaffe, M. P. (1990) *J. Cell Biol.* **111,** 967–976.
13. Sogo, L. F. & Yaffe, M. P. (1994) *J. Cell Biol.* **126,** 1361–1373.
14. Nurse, P. (1994) *Mol. Biol. Cell.* **5,** 613–616.
15. Snell, V. & Nurse, P. (1994) *EMBO J.* **13,** 2066–2074.
16. Verde, F., Mata, J. & Nurse, P. (1995) *J. Cell Biol.* **131,** 1529–1538.
17. Nurse, P., Thuriaux, P. & Nasmyth, K. (1976) *Mol. Gen. Genet.* **146,** 167–178.
18. Nasmyth, K. & Nurse, P. (1981) *Mol. Gen. Genet.* **182,** 119–124.
19. Moreno, S., Klar, A. & Nurse, P. (1991) *Methods Enzymol.* **194,** 795–823.
20. Hagan, I. M. & Hyams, J. S. (1988) *J. Cell Sci.* **89,** 343–357.
21. Harlow, E. & Lane, D. (1988) *Antibodies: A Laboratory Manual* (Cold Spring Harbor Lab. Press, Plainview, NY).
22. Jensen, R. E. & Yaffe, M. P. (1988) *EMBO J.* **7,** 3863–3871.
23. Woods, A., Sherwin, T., McRae, T. H., Baines, A. J. & Gull, K. (1989) *J. Cell Sci.* **93,** 491–500.
24. Bereiter-Hahn, J. (1976) *Biochim. Biophys. Acta* **423,** 1–14.
25. Miyakawa, I., Aoi, H., Sando, N. & Kuroiwa, T. (1984) *J. Cell Sci.* **66,** 21–38.
26. Strieiblova, E. & Wolf, A. (1972) *Z. Allg. Mikrobiol.* **12,** 673–684.
27. Toda, T., Adachi, Y., Hiraoka, Y. & Yanagida, M. (1984) *Cell* **37,** 233–242.
28. Adachi, Y., Toda, T., Niwa, O. & Yanagida, M. (1986) *Mol. Cell. Biol.* **6,** 2168–2178.
29. Hiraoka, Y., Toda, T. & Yanagida, M. (1984) *Cell* **39,** 349–358.
30. Toda, T., Umesono, K., Hirata, A. & Yanagida, M. (1983) *J. Mol. Biol.* **168,** 251–270.
31. Ayscough, K., Hajibagheri, N. M. A., Watson, R. & Warren, G. (1993) *J. Cell Sci.* **106,** 1227–1237.
32. Steinberg, G. & Schliwa, M. (1993) *J. Cell Sci.* **106,** 555–564.
33. Kilmartin, J. V. & Adams, A. E. M. (1984) *J. Cell Biol.* **98,** 922–933.
34. Adams, A. E. M. & Pringle, J. R. (1984) *J. Cell Biol.* **98,** 934–945.
35. Vale, R. D. (1987) *Annu. Rev. Cell Biol.* **3,** 347–378.
36. Hagan, I. & Yanagida, M. (1992) *Nature (London)* **356,** 74–76.
37. Goldstein, L. S. B. (1993) *Annu. Rev. Genet.* **27,** 319–351.